

2009

Low-temperature metamagnetic states in single crystal TbNi₂B₂C studied by torque magnetometry

K. D. D. Rathnayaka
Texas A&M University

D. G. Naugle
Texas A&M University

B. I. Belevtsev
National Academy of Sciences of Ukraine

Paul C. Canfield
Iowa State University, canfield@ameslab.gov

Sergey L. Bud'ko
Iowa State University, budko@ameslab.gov
Follow this and additional works at: http://lib.dr.iastate.edu/ameslab_pubs

 Part of the [Condensed Matter Physics Commons](#)

The complete bibliographic information for this item can be found at http://lib.dr.iastate.edu/ameslab_pubs/205. For information on how to cite this item, please visit <http://lib.dr.iastate.edu/howtocite.html>.

This Article is brought to you for free and open access by the Ames Laboratory at Iowa State University Digital Repository. It has been accepted for inclusion in Ames Laboratory Publications by an authorized administrator of Iowa State University Digital Repository. For more information, please contact digirep@iastate.edu.

Low-temperature metamagnetic states in single crystal TbNi₂B₂C studied by torque magnetometry

Abstract

Metamagnetic transitions in single crystal TbNi₂B₂C have been studied at 1.9 K with a Quantum Design torque magnetometer. The critical fields for the transitions depend strongly on the angle between the applied field and the easy axis [100]. Torque measurements have been made while changing the angular direction of the magnetic field (parallel to basal tetragonal ab-planes) at fixed field magnitude and while changing the field magnitude at fixed angular direction over a wide angular range (more than two quadrants). Torque magnetometry (sensitive only to the component of magnetization perpendicular to the field) indicates not only a different sequence of metamagnetic phases for fields near the easy axis from those near the hard axis, but also the different natures of a principal metamagnetic phase near the hard axis. Comparison of the results with longitudinal magnetization measurements is presented.

Keywords

Physics and Astronomy, Torque, Metamagnetism, Torque measurement, Magnetization measurement, Critical fields

Disciplines

Condensed Matter Physics

Comments

The following article appeared in *Journal of Applied Physics* 105 (2009): 07E111 and may be found at <http://dx.doi.org/10.1063/1.3062829>.

Rights

Copyright 2009 American Institute of Physics. This article may be downloaded for personal use only. Any other use requires prior permission of the author and the American Institute of Physics.

Low-temperature metamagnetic states in single crystal TbNi₂B₂C studied by torque magnetometry

K. D. D. Rathnayaka, D. G. Naugle, B. I. Belevtsev, P. C. Canfield, and S. L. Budko

Citation: *Journal of Applied Physics* **105**, 07E111 (2009); doi: 10.1063/1.3062829

View online: <http://dx.doi.org/10.1063/1.3062829>

View Table of Contents: <http://scitation.aip.org/content/aip/journal/jap/105/7?ver=pdfcov>

Published by the [AIP Publishing](#)

Articles you may be interested in

[Magnetoresistivity and anisotropy along c-axis of ErNi₂B₂C](#)

J. Appl. Phys. **107**, 09E132 (2010); 10.1063/1.3373297

[Investigation of compounds for magnetocaloric applications: YFe₂H_{4.2}, YFe₂D_{4.2}, and Y_{0.5}Tb_{0.5}Fe₂D_{4.2}](#)

J. Appl. Phys. **105**, 013914 (2009); 10.1063/1.3055348

[Torque magnetometry studies of new low temperature metamagnetic states in ErNi₂B₂C](#)

J. Appl. Phys. **103**, 07B718 (2008); 10.1063/1.2829034

[Metamagnetic transitions in RFe₂\(H, D\)_{4.2} compounds \(R = Y, Tb\)](#)

J. Appl. Phys. **101**, 09G514 (2007); 10.1063/1.2710456

[Superconductivity and normal state properties of non-centrosymmetric CePt₃Si: a status report](#)

Low Temp. Phys. **31**, 748 (2005); 10.1063/1.2008135



AIP | Journal of Applied Physics

Journal of Applied Physics is pleased to announce **André Anders** as its new Editor-in-Chief

Low-temperature metamagnetic states in single crystal $\text{TbNi}_2\text{B}_2\text{C}$ studied by torque magnetometry

K. D. D. Rathnayaka,^{1,a)} D. G. Naugle,^{1,b)} B. I. Belevtsev,² P. C. Canfield,³ and S. L. Budko³

¹Department of Physics, Texas A&M University, College Station, Texas 77843, USA

²B. Verkin Institute for Low Temperature Physics and Engineering, National Academy of Sciences, Prospekt Lenina 47, Kharkov 61103, Ukraine

³Ames Laboratory and Department of Physics and Astronomy, Iowa State University, Ames, Iowa 50011 USA

(Presented 12 November 2008; received 17 September 2008; accepted 27 October 2008; published online 12 February 2009)

Metamagnetic transitions in single crystal $\text{TbNi}_2\text{B}_2\text{C}$ have been studied at 1.9 K with a Quantum Design torque magnetometer. The critical fields for the transitions depend strongly on the angle between the applied field and the easy axis [100]. Torque measurements have been made while changing the angular direction of the magnetic field (parallel to basal tetragonal ab -planes) at fixed field magnitude and while changing the field magnitude at fixed angular direction over a wide angular range (more than two quadrants). Torque magnetometry (sensitive only to the component of magnetization perpendicular to the field) indicates not only a different sequence of metamagnetic phases for fields near the easy axis from those near the hard axis, but also the different natures of a principal metamagnetic phase near the hard axis. Comparison of the results with longitudinal magnetization measurements is presented. © 2009 American Institute of Physics.

[DOI: 10.1063/1.3062829]

The rare-earth nickel borocarbides $R\text{Ni}_2\text{B}_2\text{C}$ (where R is a rare-earth element) provide a unique family for studies of a wide range of research themes in correlated electron systems: coexistence of superconductivity and magnetism, heavy fermion behavior, nonlocality and flux line lattice transitions, and complex metamagnetism (see reviews¹⁻⁴). For $R = \text{Er}-\text{Tb}$ there is large magnetic anisotropy associated with the crystal electric field splitting of Hund's rule ground state J -multiplet with the local moment confined to the basal plane of the tetragonal unit cell. The large magnetic anisotropy restricts the local moment for both $R = \text{Er}$ and Tb to lie along the easy [100] axes. Although for $R = \text{Er}$ antiferromagnetism coexists with superconductivity, the $R = \text{Tb}$ compound with $T_N \approx 15$ K (Refs. 5 and 6) does not exhibit superconductivity, at least above 0.3 K.⁷ For both the $R = \text{Er}, \text{Tb}$ compounds the magnetic phases for $H = 0$ are spin-density wave (SDW) states with modulation vector $\mathbf{Q} = f\mathbf{a}^*$ (or \mathbf{b}^* where $\mathbf{a}^*, \mathbf{b}^*$ are reciprocal lattice vectors) with $f \approx 0.55$ and with the ordered moments perpendicular to \mathbf{Q} for Er and parallel to \mathbf{Q} for Tb , indicative of Fermi-surface nesting effects. Below $T_{WF} (\approx 2.5$ K for Er and ≈ 8 K for Tb) both systems appear to exhibit weak ferromagnetism believed to be associated with a commensurate SDW lock-in transition.⁸

Each magnetic member of the $R\text{Ni}_2\text{B}_2\text{C}$ family exhibits a fascinating series of metamagnetic transitions as displayed in longitudinal magnetization measurements.⁹ For $\text{TbNi}_2\text{B}_2\text{C}$ the phase diagram from these measurements indicates a series of four (one at $H \approx 1.2$ T and three closely spaced between ≈ 2 T and 2.7 T) metamagnetic transitions (i.e., four

metamagnetic phases) as the field applied along an easy [100] axis is increased to progress from the weak ferromagnetic (WFM) phase to the saturated paramagnetic phase. The saturation magnetization for H along that axis was observed to increase for each of the four subsequent phases with the magnetization for the saturated paramagnet about $9.6\mu_B/\text{Tb}$. For H applied near a hard axis [110] only three transitions are observed: the first representing an extension of the lowest field transition observed with H along [100], i.e., $\theta = 0$, the second to a new phase, and the third with the critical field diverging as the field direction approaches [110]. The three closely spaced transition boundaries appear to merge for fields at an angle θ to the easy axis somewhere between 25° and 35° . Torque magnetometry studies,^{10,11} which are naturally sensitive only to the component of the magnetization perpendicular to the applied magnetic field, have recently provided new insight to some of these metamagnetic phases for $R = \text{Ho}, \text{Er}$ and these may clarify the picture for Tb . Here a low temperature ($T \approx 1.9$ K) study of the metamagnetic phases in $\text{TbNi}_2\text{B}_2\text{C}$ by torque magnetometry is presented.

In this work, a physical property measurement system (PPMS) 550 (see the description in Ref. 12) torque magnetometer is used to study angular dependence of the metamagnetic phases in $\text{TbNi}_2\text{B}_2\text{C}$. It measures the torque $\vec{\tau} = \mathbf{M} \times \mathbf{H}$ so that $\tau = MH \sin(\beta)$, where β is the angle between the external field (H) and the magnetization (M). A small, somewhat irregular shaped (maximum dimensions $0.37 \times 0.32 \times 0.25$ mm³) single crystal platelet sample (about 0.05 mg) cut with the c -axis along the long dimension was mounted on the PPMS torque chip which had a rms torque noise level about 1×10^{-9} N m and a maximum allowable torque of about 5×10^{-5} N m. The chip was mounted on the PPMS

^{a)}Electronic mail: daya@tamu.edu.

^{b)}Electronic mail: naugle@physics.tamu.edu.

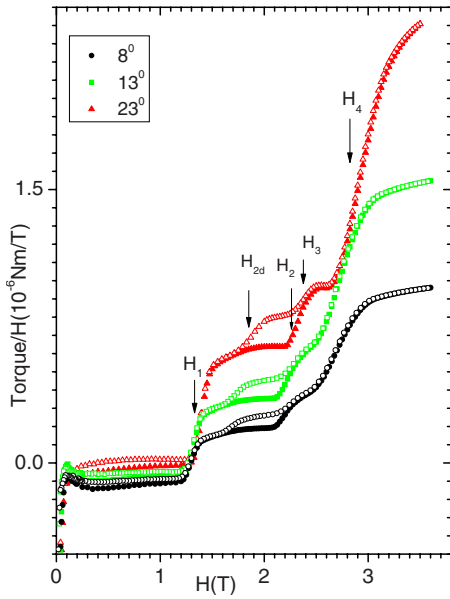


FIG. 1. (Color online) Dependences $\tau(H)/H$ at $T=1.9$ K for increasing and decreasing magnetic field (filled and empty symbols, respectively) for field directions close to an easy axis $\theta \approx 8^\circ$ (circles), $\approx 13^\circ$ (squares), and $\approx 23^\circ$ (triangles). Positions for the transition fields for $\theta \approx 23^\circ$ are shown by arrows.

rotator so that the field lies in the crystal *ab*-plane with the measured torque along the *c*-axis. Estimates of demagnetization effects indicate a negligible influence on the error in determination of the transition fields. The single crystal was grown from a Ni_2B flux in Canfield’s laboratory, and transport measurements made in Naugle’s laboratory with pieces of the same crystal were in agreement with other published results for similar single crystals of $\text{TbNi}_2\text{B}_2\text{C}$. Torque measurements were made in Naugle’s laboratory both as a function of magnitude of the magnetic field at a fixed angle of the field relative to the crystal axes and as a function of angle between the field and the crystal axes at constant field. In some cases the torque was sufficiently large that the torque chip rotated a few degrees toward the magnetic field so that the angle on the rotator did not actually reflect the orientation of the sample with respect to the applied field. These data were corrected using the chip torque constant, $K=3 \times 10^{-6}$ N m/deg for plots of the metamagnetic phase boundaries.

The metamagnetic transitions manifest themselves as sharp changes in the field dependence of $\tau(H)/H$ at critical fields, as shown in Figs. 1 and 2 for different angles θ between \vec{H} and $[100]$ axis. The angular phase diagram obtained for $\text{TbNi}_2\text{B}_2\text{C}$ is shown in Fig. 3. The critical fields were defined as the inflection points of the $\tau(H)/H$ curves found using the derivatives. Where there was significant hysteresis, the boundaries for increasing and decreasing fields are both shown.

As seen in Fig. 1, τ/H for $\theta \approx 8^\circ$, 13° , and 23° (i.e., near an easy axis) shows a series of three plateaus for increasing and four for decreasing field for $H > 1$ T. The data below $H \approx 1$ T appear to be related to the weak ferromagnet phase, and the four plateaus correspond to the four metamagnetic phases observed in the longitudinal magnetization.⁹ The tran-

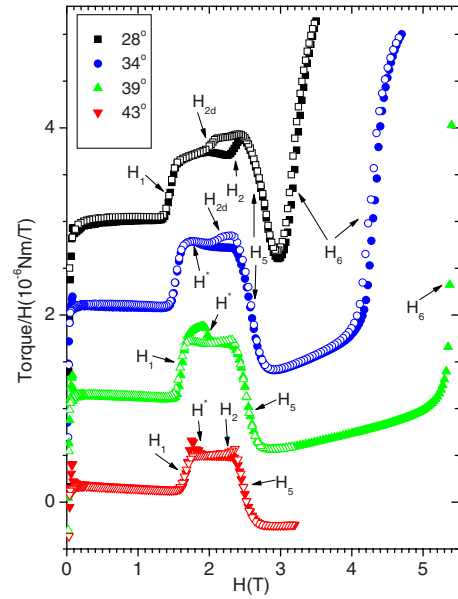


FIG. 2. (Color online) $\tau(H)/H$ dependence at $T=1.9$ K for increasing and decreasing field (filled and empty symbols, respectively) for field directions close to a hard axis: $\theta \approx 28^\circ$, $\theta \approx 34^\circ$, $\theta \approx 39^\circ$, and $\theta \approx 43^\circ$. Positions of transitions fields are marked by arrows. The τ/H scale corresponds to the $\theta=43^\circ$ while the other curves have been shifted by 10^{-6} N m/T, successively, for clarity.

sition fields H_i , $i=1-4$, are marked for the increasing field data at 23° by arrows. For decreasing fields H_{2d} is also marked. It is quite clear from the data in Fig. 1 that there is only significant hysteresis for the second transition, so that the second (at the field marked by H_2) and third (at the field

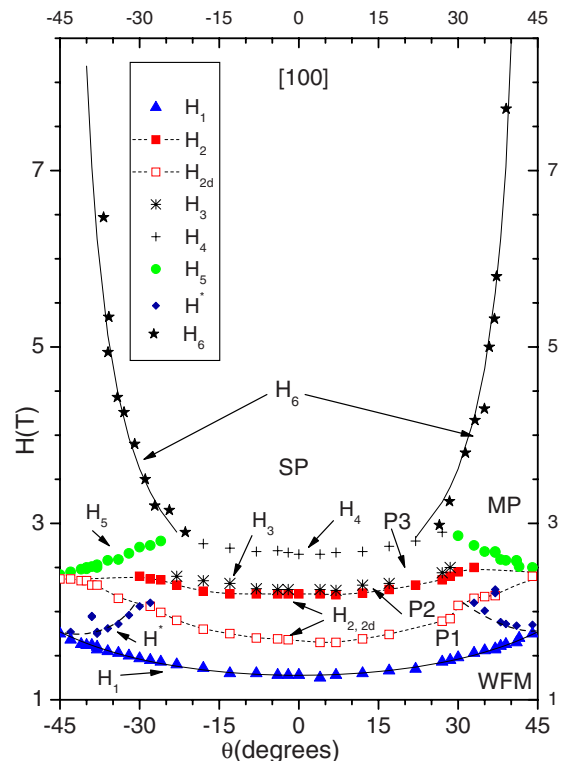


FIG. 3. (Color online) Angular phase diagram of metamagnetic states at $T=1.9$ K. Solid curves are fits to the boundary while dashed ones are guides to the eye. Critical fields are labeled per text. Open symbols for H_{2d} are from data with decreasing field. H_2 corresponds to data from increasing field.

marked by H_3) transitions appear to proceed continuously for increasing field (solid symbols). Except for the very large hysteresis reported here for H_2 the torque and longitudinal magnetization results⁹ are in reasonable agreement.

Figure 2 shows τ/H for angles $\theta \approx 28^\circ, 34^\circ, 39^\circ$, and 43° (near the hard axis) and provides new insight into the metamagnetic phases previously reported. In the curves for $\theta \approx 28^\circ, 34^\circ$, and 39° four transitions marked by arrows labeled H_1, H_2, H_5 , and H_6 are clearly shown. For $\theta \approx 43^\circ$, the last transition H_6 is not shown since it is at much higher field. This last transition H_6 is to the saturated paramagnetic state, and its critical field diverges near the hard axis. It corresponds to the diverging phase boundary indicated by the final small increase in magnetization in superconducting quantum interference device measurements⁹ for increasing field applied at angles near a hard axis. For the third transition at H_5 , the torque decreases and changes sign indicative of a rotation of the net magnetization to lie along the hard axis. This is also confirmed by τ/H curves taken at fixed field as a function of θ (not shown). This is consistent with a mixed phase of approximately equal contributions from two phases each with magnetization along the two nearest easy axes as discussed further below. The transition labeled by H_2 and H_{2d} (decreasing H) for $\theta = 28^\circ$ is very hysteretic and is thought to be a continuation of H_2 from the region with H near an easy axis. For angles within about 15° either side of the hard axis ($\theta = \pm 45^\circ$) a new phase boundary H^* marked by a very small decrease in τ/H as H is increased is seen. This is most easily seen for $\theta = 39^\circ$ and $\theta = 43^\circ$ in Fig. 2. The small decrease in τ/H suggests a small rotation of the net magnetization from the nearest easy axis toward the hard axis. This is perhaps a result of frustration effects for fields near the hard axis. No indication of this transition was observed in longitudinal magnetization since it would produce a negligible change in the component along the field.

The resulting phase diagram from torque measurements shown in Fig. 3 is similar to that shown in Ref. 8, with the exceptions that the large hysteresis for the transition H_2 is indicated by critical fields H_2 and H_{2d} (increasing, decreasing H , respectively) in Fig. 3 and that a new phase boundary marked by H^* appears between H_1 and H_2 for angles within about 15° on either side of a hard axis ([110], $\theta = 45^\circ$). It appears to represent a small rotation of M . The phases WFM, P1, P2, P3 (metamagnetic phases that exist for fields not too close to the hard axis), SP (the saturated paramagnetic phase), and MP (probably a mixed phase where the net magnetization lies rather precisely along the hard axis as shown by the torque measurements) were all indicated by the longitudinal magnetization measurements.⁹ The fit to the data in

Fig. 3 for the boundary $H_1(\text{kOe}) \approx 11.9/\cos(\theta) + 0.9$ is comparable to $12.1/\cos(\theta)$ in Ref. 8. The boundary between MP and SP in Fig. 3 has been fit by $H_6 \approx 0.6/\sin(\phi) + 1.3$ T, where ϕ is the angle between H and the hard axis. The hysteresis in H_2 is quite strong, at least for the normal component of M as measured in torque magnetometry, as shown in Fig. 3.

The most important result from this torque magnetometry study is that the high field phase (MP) near the hard axis bounded by H_5 and H_6 has the net magnetization aligned rather precisely along the hard axis. This could represent a single modulated phase, but more likely it is a mixture of two frustrated phases with the magnetization of each directed along different nearest easy axes. A similar phase was identified for both $R=\text{Ho}$ and Er borocarbides by torque magnetometry.^{10,11}

In summary, torque magnetization measurements basically confirm the metamagnetic phase diagram for $\text{TbNi}_2\text{B}_2\text{C}$ determined by longitudinal magnetization measurements, but with the addition of a new phase representing a small rotation of the magnetization at intermediate fields near the hard axis. The torque measurements also clearly indicate that the magnetization of the high field phase for H near the hard axis lies along that axis and is most likely a mixed phase resulting from frustration as observed for the corresponding Er and Ho intermetallic compounds.

The research at TAMU was supported by the Robert A. Welch Foundation (No. A-0514). Ames Laboratory is operated for the U.S. Department of Energy by Iowa State University under Contract No. W-7405-Eng.-82 and work there is supported by the Director for Energy Research, Office of Basic Energy Sciences.

¹S. L. Budko and P. C. Canfield, *C. R. Phys.* **7**, 56 (2006).

²L. C. Gupta, *Adv. Phys.* **55**, 691 (2006).

³K.-H. Müller and V. N. Narozhnyi, *Rep. Prog. Phys.* **64**, 943 (2001).

⁴D. G. Naugle, K. D. D. Rathnayaka, and A. K. Bhatnagar, in *Studies of High Temperature Superconductors*, edited by A. Narlikar (Nove Science, New York, 1999), Vol. 28, pp. 199–239.

⁵B. K. Cho, P. C. Canfield, and D. C. Johnson, *Phys. Rev. B* **53**, 8499 (1996).

⁶P. Dervenagas, J. Zarestky, C. Stasis, A. I. Goldman, P. C. Canfield, and B. K. Cho, *Phys. Rev. B* **53**, 8506 (1996).

⁷C. V. Tomy, J. M. Martin, D. McK. Paul, *Physica B* **223–224**, 116 (1996).

⁸F. Bourdarot, J. W. Lynn, E. Baggio-Saitovitch, Q. Huang, D. R. Sanchez, and S. Skanthakumar, *Phys. Rev. B* **64**, 104410 (2001).

⁹P. C. Canfield and S.L. Budko, *J. Alloys Compd.* **262–263**, 169 (1997).

¹⁰K. D. D. Rathnayaka, B. I. Belevtsev, and D. G. Naugle, *Phys. Rev. B* **76**, 224526 (2007).

¹¹D.G. Naugle, B.I. Belevtsev, K.D. D. Rathnayaka, S.-I. Lee, S.M. Yeo, *J. Appl. Phys.* **103**, 07B718 (2008).

¹²See: <http://www.qdusa.com/products/ppms.html>.